

Superconducting quantum interference phenomenon in $\text{Bi}_2\text{Sr}_2\text{CaCu}_2\text{O}_{8+\delta}$ single crystals

M. Sandberg¹ and V. M. Krasnov^{2*}

¹ *Department of Microtechnology and Nanoscience,*

Chalmers University of Technology, SE-41296 Göteborg, Sweden

² *Department of Physics, Stockholm University,*

Albanova University Center, SE-10691 Stockholm, Sweden

(Dated: November 6, 2018)

The operational dc-SQUID based on intrinsic Josephson junctions in $\text{Bi}_2\text{Sr}_2\text{CaCu}_2\text{O}_{8+\delta}$ high- T_c superconductor is fabricated and studied. The novel in-plane loop layout and the developed in-situ endpoint detection method allowed an accurate control of the number of junctions in the SQUID. A clear periodic modulation of the superconducting current as a function of magnetic flux through the SQUID loop is observed. This is an unambiguous evidence for the quantum interference phenomenon in $\text{Bi}_2\text{Sr}_2\text{CaCu}_2\text{O}_{8+\delta}$ single crystals.

PACS numbers: 85.25.Dq, 74.72.Hs, 74.50.+r

Atomic scale "intrinsic" Josephson junctions (IJJ's) are naturally formed in layered high- T_c superconductors such as the $\text{Bi}_2\text{Sr}_2\text{CaCu}_2\text{O}_{8+\delta}$ (Bi-2212) [1, 2, 3, 4, 5, 6, 7, 8]. IJJ's can be employed as building blocks for various cryoelectronic devices [5, 6]. Record-large I_cR_n values $\sim 10\text{-}15$ mV make them particularly attractive for high frequency applications [2, 5]. IJJ's are perfect for 3D-integration of many junctions. Operating 3D quantum devices containing 11000 IJJ's were already demonstrated [5]. Moreover, properties of IJJ's can be controlled in a wide range by changing O-doping [9], temperature, magnetic field and intercalation [7]. This is important for device applications and may allow tunability similar to band engineering in semiconducting quantum devices [10].

The Superconducting Quantum Interference Device (SQUID) is one of the most important and widely used cryoelectronic devices [11], both due to its extreme sensitivity used in

*Electronic address: vladimir.krasnov@physto.se

various types of sensors, and as a basis element for digital Josephson electronics [12].

Operation of a dc-SQUID, based on IJJ's, was analyzed in Ref.[13]. Since the interlayer spacing $\simeq 15\text{\AA}$ in Bi-2212 is very small, such an "intrinsic" SQUID will contain several stacked IJJ's in each arm. It is known that operation of a multi-junction SQUID is complicated due to existence of metastable states and a small current-flux modulation [14]. Basically, the same is true for a stacked SQUID, even though some improvement can be achieved [13] in case of phase-locking of IJJ's in the stack [15]. Anyway, the current-flux modulation of the stacked SQUID decreases roughly inversely proportional to the number of junctions [13]. Therefore, SQUID's should have as few and as identical IJJ's as possible to have the best performance. In the previous attempt, a 3D Focused Ion Beam (FIB) sculpturing was used to fabricate the intrinsic SQUID with the out-of-plane (in the bc -plane) loop. The SQUID contained a large amount of junctions and no interference pattern could be observed [16].

Here we report on successful fabrication of operational Bi-2212 intrinsic dc-SQUID with the novel in-plane loop layout, made by double-side patterning and FIB milling. The progress was achieved by developing an accurate end-point detection technique, which allowed fabrication of the SQUID with only few IJJ's. The fabricated device shows periodic modulation of the superconducting current as a function of applied magnetic field, which is a clear evidence for the quantum interference phenomenon in Bi-2212 single crystals [17].

Fig. 1a) shows a layout of the intrinsic dc-SQUID with the in-plane loop [13]. Here the SQUID loop is placed in the ab -plane and stacks of IJJ's are formed by etching trenches from top and bottom sides of the crystal.

Figs. 1 b,c) show a secondary electron- and a back-illumination optical images, respectively, of the actual intrinsic dc-SQUID studied in this work. The fabrication procedure required a double side fabrication technique [5] and consisted of five major steps:

- i) A Bi-2212 crystal was glued to a sapphire substrate using hard baked photoresist, the top part was cleaved-off using adhesive tape and 30 nm of Au was deposited to prevent surface deterioration.
- ii) A large mesa structure $120 \times 120\mu\text{m}^2$ with a hight of $\sim 0.5\mu\text{m}$ was etched on top of the crystal by wet chemical etching. A bottom trench, line - (C) in Fig. 1 b), was etched using a combination of argon ion milling and wet chemical etching in a saturated EDTA solution.

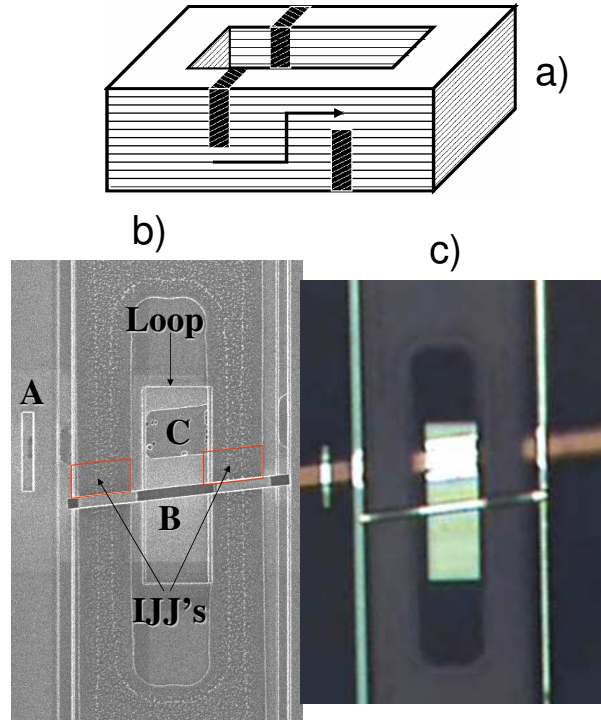


FIG. 1: a) The layout of intrinsic dc-SQUID with in-plane loop. The current is forced to flow in the *c*- axis direction by trenches from top and bottom sides of SQUID arms. b) SEM image of the SQUID: A - the small window used for endpoint detection. B- the top trench, C- the bottom trench seen through the loop hole. c) back-illumination optical image of the same SQUID. Etched parts are seen as bright areas. The parameters of the SQUID are: the loop size $20 \times 7 \mu m^2$, the IJJ stack sizes in both arms $\sim 5 \times 3 \mu m^2$.

- iii) The crystal was flipped and glued to a new substrate with the mesa facing down.
- iv) The crystal was cleaved-off, leaving only the large mesa on the substrate. A metallization gold layer was deposited. The SQUID loop, electrodes and contact pads were formed by photolithography and argon ion milling. Three SQUID's were made on each chip.
- v) The sample was transferred to a standard FIB. The loop and the top trench, line - (B) in Fig. 1 b), were made by FIB. In addition, FIB-cuts were made to separate SQUID's made on the same crystal, see vertical bright lines in Fig. 1 c). Stacks of IJJ's, restricted by the bottom and the top trenches, were formed in each arm of the SQUID loop, see areas marked (IJJ's) in Fig. 1 b) and the layout in Fig. 1 a).

The main challenge for fabrication of the SQUID is an accurate control of the number of IJJ, N , in each arm of the SQUID. N is proportional to the overlap between top and

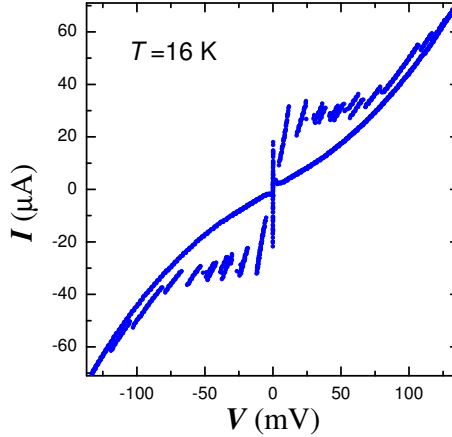


FIG. 2: The IVC of the dc-SQUID, shown in Fig.1, at $T \simeq 16K$. There are six plus one regular quasiparticle branches and a number of tiny ghost sub-branches caused by parallel connection of the two slightly different stacks of IJJs. The number of IJJ's in each stack $N = 6 + 1$.

bottom trenches. To minimize N etching of the top trench should be stopped as soon as it reaches the level of the bottom trench. To do this we developed a simple endpoint detection method: a test line with the same width as the top trench was milled simultaneously with the top trench in the area above the bottom trench, outside the SQUID, see the line - A in Fig. 1 b). When the test line was etched down to the bottom trench, secondary electron emission, monitored during FIB-milling, was reduced and etching was terminated. The contrast between etched (darker) and unetched areas within the test line is clearly seen in Fig. 1 b). This simple endpoint detection method provided an accuracy of \sim few IJJ's.

Fig. 2 shows the Current-Voltage characteristics (IVC) at $T \simeq 16K$ for the same SQUID. The IVC was measured in the four-probe/superconducting two-probe configuration, avoiding the contact resistance. A multi-branch structure due to one-by-one switching of IJJ's from the superconducting into the resistive state is seen. Counting the number of branches we conclude that the SQUID contains $N = 6$ stacked IJJ's with the critical current $I_c \simeq 15 - 20\mu A$ and one larger junction with $I_c \simeq 25 - 30\mu A$, which, however, remained in the superconducting state during experiments discussed below.

In Fig. 2 we can also see tiny "ghost" sub-branches, which sometimes are also seen

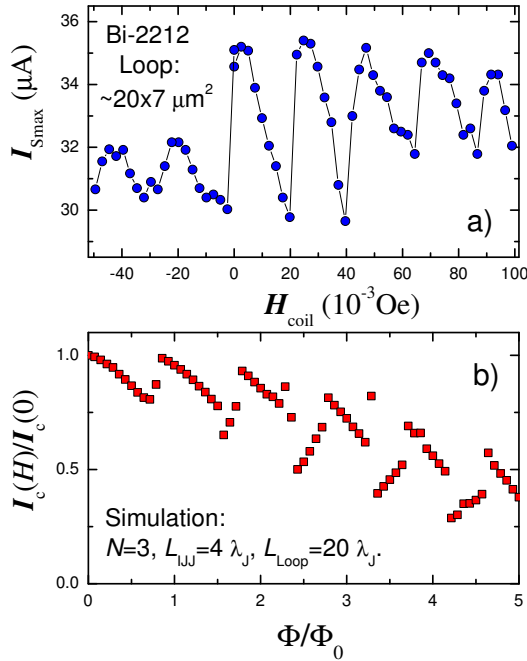


FIG. 3: a) Modulation of the most probable switching current as a function of applied magnetic field, for the same SQUID as in Figs.1, 2 at $T \simeq 4.2\text{K}$. Periodic modulation clearly indicates the quantum interference phenomenon. b) Numerically simulated current-flux modulation for a dc-SQUID with $N = 3$ identical stacked IJJ's in each arm. A characteristic saw-tooth like modulation is seen (data from Ref. [13]).

in single stack mesas and are due to non-uniformity of junctions [18]. However, the sub-branches in SQUID's are much more pronounced than in mesas. This is probably due to parallel connection of stacks with slightly different areas and critical currents. Each time an extra IJJ switches into the resistive state in one of the stacks, the current distribution between the arms of the SQUID has to be re-adjusted to maintain the same voltage across both stacks.

Fig. 3 a) shows the measured dependence of the most probable switching current, I_{Smax} , on magnetic field, applied perpendicular to the SQUID loop at $T \simeq 4.2\text{K}$, for the same device. To obtain I_{Smax} , 30720 switching events from the superconducting to the resistive state were measured using sample-and-hold technique [8]. This was done to reduce ambiguity caused by thermal fluctuations, which were significant in this device due to a small value of I_c .

A clear periodic modulation of the switching current vs. the applied magnetic field is

seen in Fig. 3. The period is several times smaller than the flux quantum divided by the loop area. This is caused by flux focusing due to a specific geometry of the device: the SQUID is surrounded by Bi-2212 crystal, seen as dark areas in Fig. 1 c). Therefore, magnetic field can penetrate only through the cuts in the crystal, seen as bright vertical lines in Fig. 1 c), resulting in strong flux focusing effect near the edges of the SQUID loop. The maximum amplitude of modulation $\sim 15\%$ is consistent with a rough estimation $\Delta I_c/I_c \sim 1/N$ for $N = 6$ IJJ's in each stack. Moreover, the characteristic saw-tooth like shape of the modulation is consistent with the numerical simulations for a stacked SQUID [13], shown in Fig. 3 b).

The in-plane SQUID loop layout, employed here has several important advantages in comparison to the out-of-plane loop layout used in the previous work [16]:

- (i) First, slow ion beam (not necessarily focused) etching in the c -axis direction, in combination with the developed endpoint detection, allows a much better control of the number of IJJ's (fabrication of a single IJJ is feasible [19]), compared to FIB etching in the ab -plane direction [16]. The number of IJJ's is the most important parameter of the intrinsic SQUID, since modulation of I_c decreases roughly as $1/N$ [13]. In our devices no modulation could be seen for $N > 20$, as it probably became less than thermal fluctuations and noise in the system.
- (ii) Second, the in-plane loop is not limited by the small thickness of Bi-2212 crystals and, therefore, can be made almost arbitrary large. The loop inductance can easily be made much larger than the inductance of IJJ's, improving SQUID performance [11]. For example, the inductance of the loop for our SQUID is more than two orders of magnitude larger than for the out-of-plane SQUID studied in Ref.[16].

In conclusion, we fabricated and studied operational intrinsic dc-SQUID made from a Bi-2212 single crystal. The observed periodic modulation of the switching current vs. the magnetic flux through the SQUID loop is a clear evidence for the quantum interference of superconducting wave functions in Bi-2212 single crystals. In total more than ten devices were studied. It was observed that the amplitude of modulation decreases rapidly with the number of IJJ's in the SQUID. Therefore, to improve the performance of the intrinsic SQUID the number of IJJ's should be further reduced. This can be done using the endpoint detection method developed here, possibly in combination with the slow Ar-ion milling technique, using which several groups have demonstrated a possibility to fabricate single

IJJ's [19]. This may open a possibility for building 3D-integrated electronic circuits based on intrinsic Josephson junctions.

Acknowledgments

The work was supported by the Swedish Research Council, grant Nr: 621-2001-3236.

- [1] R.Kleiner, et al, *Phys. Rev. Lett.* **68** 2394 (1992)
- [2] W.Walkenhorst et al., *Phys. Rev. B* **56**, 8396 (1997)
- [3] K. Schlenga et al., *Phys. Rev. B* **57**, 14518 (1998)
- [4] V.M. Krasnov et al., *Phys.Rev.B* **59**, 8463 (1999);
- [5] H.B.Wang et al., *Appl. Phys. Lett.* **77**, 1017 (2000)
- [6] Yu.I.Latyshev, et al., *Physica C* **362** 165 (2001)
- [7] V.M. Krasnov et al., *Phys.Rev.Lett.* **84**, 5860 (2000); *ibid.* **86**, 2657 (2001)
- [8] V.M. Krasnov, et. al., *cond-mat* /0501664
- [9] K. Inomata, et al., *Appl.Phys.Lett.* **82**, 769 (2003); V.M. Krasnov, *Phys.Rev.B* **65**, 140504(R) (2002).
- [10] J.Faist, et al., *Science* **264** (1994) 553
- [11] D.Koelle et al., *Rev. Mod. Phys* **71** 631 (1999)
- [12] H.Hyakawa, et al., *Proc. IEEE* **92** 1549 (2004); O.A.Mukhanov, et al., *Proc. IEEE* **92** 1564 (2004)
- [13] V.M. Krasnov, *Physica C* **368**, 246 (2002)
- [14] S.J. Lewandowski, *Phys. Rev. B* **43** (1992) 7776.
- [15] N.Mros et al., *Phys. Rev. B*, **57** (1998) R8135
- [16] S.-J. Kim et al., *Physica C* **412-414**, 1401 (2004)
- [17] This work is a part of the M.Sc. thesis of M.Sandberg, (Chalmers University of Technology, May 2004 Göteborg). At the final stage of preparation of this manuscript we noticed about another work in which a similar SQUID layout was employed: A.Irie et al., unpublished (NS/CTC/PLASMA-2004, November 2004 Tsukuba).
- [18] V.M. Krasnov, *Physica C* **372-376**, 103 (2002)

[19] A. Yurgens *et al.*, *Appl. Phys. Lett.* **70** 1760 (1997); Y.J.Doh, *et al.*, *Phys. Rev. B* **61** 3620 (2000); P.H.Wu, *et al.*, *Physica C* **405** 65 (2004) L.X.You *et al.*, *Supercond. Sc. Techn.* **17** 1160 (2004).